JOURNAL OF QUATERNARY SCIENCE (2010) **25**(3) 237–242

Published online 11 November 2009 in Wiley InterScience
(www.interscience.wiley.com) DOI: 10.1002/jqs.1344

Rapid Communication

Holocene bipolar climate seesaw: possible subtle evidence from the deep North East Atlantic Ocean?

MARK A. MASLIN[1]* and CHRISTOPHER W. SMART[2]
[1] Department of Geography, University College London, London, UK
[2] School of Geography, Earth and Environmental Sciences, University of Plymouth, Plymouth, UK

Maslin, M. A. and Smart, C. W. 2010. Holocene bipolar climate seesaw: possible subtle evidence from the deep North East Atlantic Ocean? *J. Quaternary Sci.*, **Vol. 25** pp. 237–242. ISSN 0267-8179.

Received 2 June 2009; Revised 27 July 2009; Accepted 17 August 2009

ABSTRACT: The occurrence of a millennial-scale bipolar climate seesaw has been documented in detail for the last glacial period and Termination. There is, however, debate whether it occurs during interglacials and if it does what influence it could have on future climate. We present here new evidence from a North East Atlantic Ocean deep-sea core which supports the hypothesis for a Holocene bipolar climate seesaw. BENGAL Site 13078#16, from the Porcupine Abyssal Plain, is 4844 m deep and situated at the North Atlantic Deep Water and Antarctic Bottom Water (AABW) interface. Planktic foraminiferal fragment accumulation rate data at this site is an indicator of coarse carbonate dissolution, which is highly sensitive to the incursion of under-saturated AABW. Five dissolution peaks have been identified, which seem to occur approximately 500 a after each of the North Atlantic 'Bond' ice rafting pulses, suggesting a subsequent subtle shallowing of AABW. This indicates a possible lagged climatic link between North East Atlantic surface water conditions and AABW production in the Southern Ocean during the Holocene. This provides the first tentative evidence that there was a Holocene bipolar climate seesaw and that the deep ocean was involved. This study also suggests that extremely sensitive locations need to be sought as the Holocene bipolar climate seesaw seems to be very subtle compared with its glacial counterparts. Copyright © 2009 John Wiley & Sons, Ltd.

Journal of Quaternary Science

KEYWORDS: Holocene; North Atlantic; bipolar climate seesaw; millennial events; deep water.

Introduction

There is clear evidence from ice core records for millennial-scale asynchronous climate variability between Antarctica and Greenland during the last glacial period (Blunier *et al.*, 1998; Blunier and Brook, 2001). This has been referred to as the bipolar climate seesaw (Broecker, 1998; Stocker, 1998) and implies a strong teleconnection between the high latitudes in the Northern and Southern Hemispheres. Various suggestions have been made to how this signal is propagated, for example internal oscillation between the dominant source of deep-water formation in the Northern *versus* Southern Hemisphere. This has been suggested to occur during glacial Dansgaard–Oeschger cycles (Vidal *et al.*, 1997; Hemming, 2004; Rasmussen and Thomsen, 2004; Schmidt *et al.*, 2006). Various driving mechanisms have been suggested to generate periodic inputs of meltwater in the North Atlantic Ocean (Seidov and Maslin, 1999, 2001; Maslin *et al.*, 2001). These freshwater inputs result in the reduction of the surface densities and periodic threshold reductions in North Atlantic Deep Water (NADW) formation. As a consequence of both the reduction of NADW and changes in cross-hemisphere heat budget balancing, Antarctic Bottom Water (AABW) expands into the North Atlantic Ocean.

Bond *et al.* (1997, 2001) have demonstrated that the Dansgaard–Oeschger millennial climate events had a persistent 1500 ± 500 a cyclicity both in the last glacial period and the Holocene. Essential to our understanding of our current interglacial climate and future climate is whether the bipolar seesaw operates during interglacial millennial climate cycles as well as glacial periods. Denton and Broecker (2008) have provide tantalising evidence that suggests there was a bipolar climate seesaw operating during the Holocene and by

* Correspondence to: M. A. Maslin, Department of Geography, University College London, Pearson Building, Gower Street, London WC1E 6BT, UK.
E-mail: mmaslin@geog.ucl.ac.uk

implication other interglacial periods. They show that for the Medieval Warm Period–Little Ice Age and 20th-century oscillations there is a link between fluctuations in Northern Atlantic Ocean red grains representing strength of the deep-water conveyor and expansion and contraction of glaciers in the Northern Hemisphere.

This study uses a marine core from the North East Atlantic Ocean, the water depth of which is currently just above the modern lower NADW–AABW boundary. Hence it is highly sensitive to small variations in these water masses over the last 10 ka. We show that there is a ca. 500 a lag between the major 'Bond' ice rafting pulses and shallowing AABW in the North East Atlantic Ocean. This is the approximate time order suggested for the effects of a meltwater pulse in the North Atlantic Ocean to propagate into the Southern Hemisphere (Schmittner *et al.*, 2003; Knutti *et al.*, 2004).

Site location

We present data which have been obtained from a 93 cm Kasten core (site 13078#16; 48° 49.91′ N, 16° 29.94′ W, water depth 4844 m) from the Porcupine Abyssal Plain (PAP), North East Atlantic, collected during RRS *Discovery* cruise 226 (April 1997) as part of the BENGAL programme (high-resolution temporal and spatial study of the BENthic biology and Geochemistry of a northeastern Atlantic abyssal Locality) (Billet and Rice, 2001) (Fig. 1). Cores at this depth in the North East Atlantic Ocean are not usually analysed in detail because the glacial sections are highly dissolved and very little carbonate remains (Sarnthein *et al.*, 1994). This is because during each glacial the NADW becomes shallower and the AABW influences this core site, dissolving much of the carbonate material raining down from the surface. At this location the deep branch of the global thermohaline circulation passes through the area (Dickson and Brown, 1994) with southward flowing Upper North East Atlantic Deep Water (NEADW, 'NADW') resulting from a mixture of Iceland–Scotland Overflow Water (ISOW) and Labrador Sea Water (LSW), and, at greater depths, northward-flowing Lower Deep Water (LDW), a component of AABW (McCartney, 1992; van Aken, 2000). AABW is under-saturated with respect to calcium carbonate and causes carbonate dissolution, whereas NADW is over-saturated and enhances carbonate preservation (Broecker and Peng, 1982; Dittert *et al.*, 1999). The level below which carbonate dissolution increases significantly is known as the calcite lysocline and occurs at the NADW/AABW boundary (Volbers and Henrich, 2002). The study site is currently situated just above the boundary between NADW and AABW and is thus extremely sensitive to changes in the position of AABW and hence is an ideal site to investigate bipolar seesaw during the Holocene.

Methods

Kasten core 13078#16 was subsampled at 2 cm intervals and studied for foraminifera. A detailed record of changes in the benthic foraminiferal faunas and benthic stable isotopes from this core are provided by Smart (2008). The age model is presented in Fig. 2 and is based on eight accelerator mass spectrometry (AMS) radiocarbon dates measured at the Leibniz Laboratory for Radiometric Dating and Stable Isotope Research, Christian-Albrechts University, Kiel, Germany, on monospecific planktic foraminiferal samples of *Globigerina bulloides* and/or *Globorotalia inflata* (errors varied from ± 30 to ± 70 a);

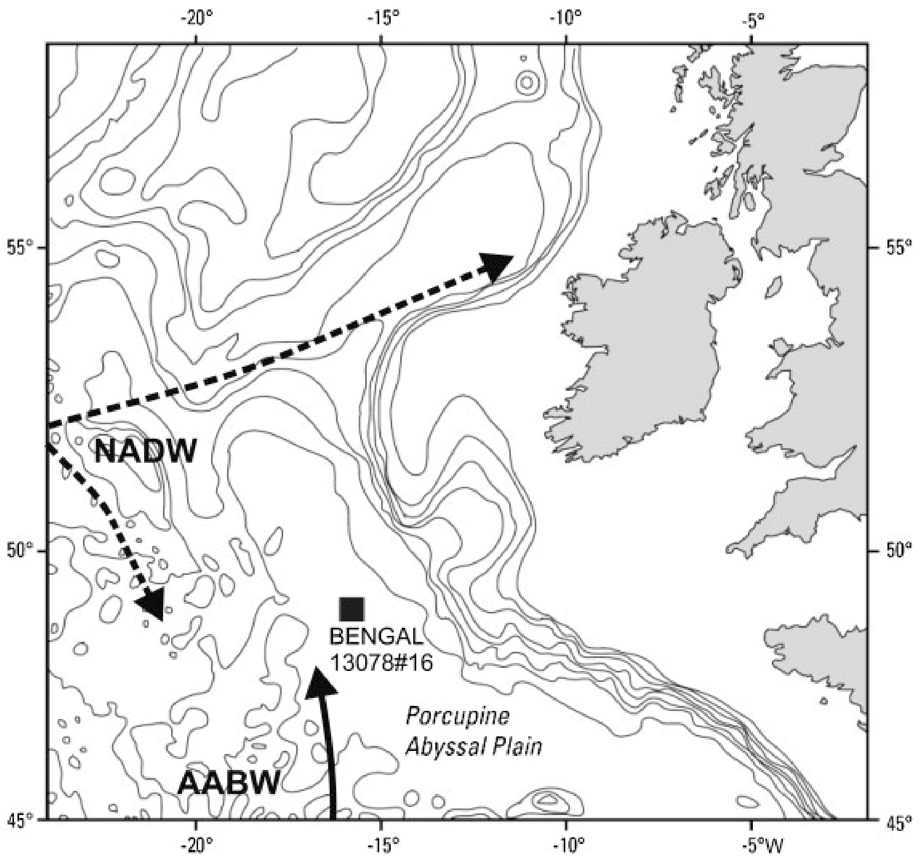

Figure 1 Location of BENGAL site 13078#16. AABW, Antarctic Bottom Water (solid arrow); NADW, North Atlantic Deep Water (dashed arrows)

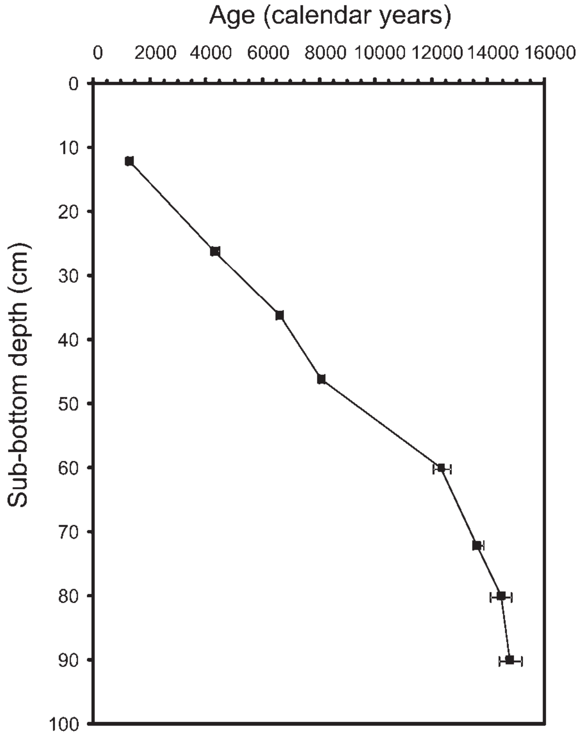

Figure 2 Age–depth plot of BENGAL site 13078#16 showing the calibrated radiocarbon dates.

see Table 1. The radiocarbon dates were converted to calendar ages (cal. a BP) using the Marine04 model (Hughen *et al.*, 2004) in OXCAL v.3.10 (Bronk Ramsey, 1995, 2001) after applying a 400 a reservoir correction. Sedimentation rates varied from 4.61 cm ka^{-1} (1.2–12.3 ka), to 9.53 cm ka^{-1} (12.5–14.4 ka), to 30.77 cm ka^{-1} (12.5–14.4 ka). Later in this paper these results are compared with those of Bond *et al.* (2001) and Bianchi and McCave (1999). The age model for the ice-rafted debris (IRD) record of Bond *et al.* (2001) was based on 45 radiocarbon dates on four cores which were then stacked into a single record. Bianchi and McCave's (1999) mean sorted silt record age model was based on 14 radiocarbon dates. Both papers applied the same 400 a reservoir correction to their radiocarbon dates before converting them to calendar years using OXCAL.

Sediment samples of approximately 4–6 g were taken from the Kasten core 13078#16 every 2 cm and were dried and weighed and a 10% sodium hexametaphosphate (Calgon) solution was added to disaggregate the samples. Samples were then washed through a >63 μm sieve, dried and weighed. For faunal abundance analysis, >250 specimens of planktic foraminifera and >250 specimens of benthic foraminifera were picked and identified from the >63 μm size fraction and the number of specimens per gram of dry sediment recorded. The percentage of *Neogloboquadrina pachyderma* (sinistral) was recorded in the >150 μm size fraction. Accumulation rates (number of specimens cm^{-2} ka^{-1}) of planktic and benthic foraminifera (>63 μm) were calculated as: number of specimens per gram of dry sediment × linear sedimentation rate (cm ka^{-1}) × dry bulk density (g cm^{-3}). The whole >63 μm fraction was dry sieved through a >150 μm sieve and the number of planktic foraminiferal fragments were counted in the whole sample. The numbers of fragments per gram (>150 μm) were recorded and the accumulation rates (>150 μm, number of specimens cm^{-2} ka^{-1}) were calculated as: number of fragments per gram of dry sediment × linear sedimentation rate (cm ka^{-1}) × dry bulk density (g cm^{-3}). We use the accumulation rates (numbers cm^{-2} ka^{-1}) of planktic foraminiferal fragments (PFAR) to document carbonate dissolution, and hence AABW variability, during the Holocene. Fragments were counted in the whole original sample (4–6 g dry weight of sediment) to remove any bias due to low counting numbers and to increase the statistical significance of the dataset. The planktic foraminiferal fragmentation index is a commonly used proxy of carbonate dissolution (Thunnell, 1976; Peterson and Prell, 1985; Le and Shackleton, 1992). However, the fragmentation index can also be influenced by relative abundance of planktic foraminiferal species and productivity (Thunnell, 1976; Le and Shackleton, 1992; Berger *et al.*, 1982).

Discussion

Five major peaks in PFAR occur during the Holocene (Fig. 3). The PFAR record was compared to complete planktic and benthic foraminiferal species assemblage counts. Prior to 12 cal. ka BP the relatively robust *Neogloboquadrina pachyderma* (sinistral coiling, *sensu* Darling *et al.*, 2006) dominates the planktic foraminiferal assemblage and this is reflected by very low PFARs. After 12 cal. ka BP the planktic foraminiferal assemblage is a diverse interglacial assemblage showing relatively little variation through the Holocene. There are no major changes in the planktic foraminiferal assemblage, particularly of fragile species between samples with peaks in PFAR and those without. Hence species effects can be ruled out for samples younger than 12 cal. ka. Benthic foraminifera were also counted in the same samples (see Smart, 2008). In the North Atlantic Ocean, it has been shown that benthic foraminiferal assemblages vary strongly with surface water productivity and the accumulation of phytodetritus (Gooday, 1988, 1996; Sun *et al.*, 2006). Planktic and benthic foraminiferal accumulation rates were also calculated, which can be interpreted as a combination of dissolution and productivity. The lack of any correspondence between the PFAR and foraminiferal accumulation rates suggests

Table 1 Radiocarbon dates and calendar year conversion for BENGAL Kastern core 13078#16

Laboratory no. (Kiel University)	Depth (cm)	Planktonic foraminifera species[a]	Conventional ^{14}C age (a BP) ± error (1σ)	Calibrated age (cal. a BP) ± error (2σ)
KIA 29120	12–13	*G. inflata*	1685 ± 30	1244.5 ± 95
KIA 29121	26–27	*G. inflata*	4200 ± 30	4279.5 ± 140
KIA 29122	36–37	*G. inflata*	6135 ± 35	6564.5 ± 135
KIA 29123	46–47	*G. inflata* + *G. bulloides*	7600 ± 45	8059.5 ± 120
KIA 29124	60–61	*G. bulloides*	10810 + 60/−55	12324.5 ± 325
KIA 29125	72–73	*G. bulloides*	12160 ± 70	13599.5 ± 180
KIA 29126	80–81	*G. bulloides*	12790 ± 70	14424.5 ± 375
KIA 29127	90–91	*G. inflata* + *G. bulloides*	12990 ± 70	14749.5 ± 400

[a] *Globigerina bulloides* and/or *Globorotalia inflata*.

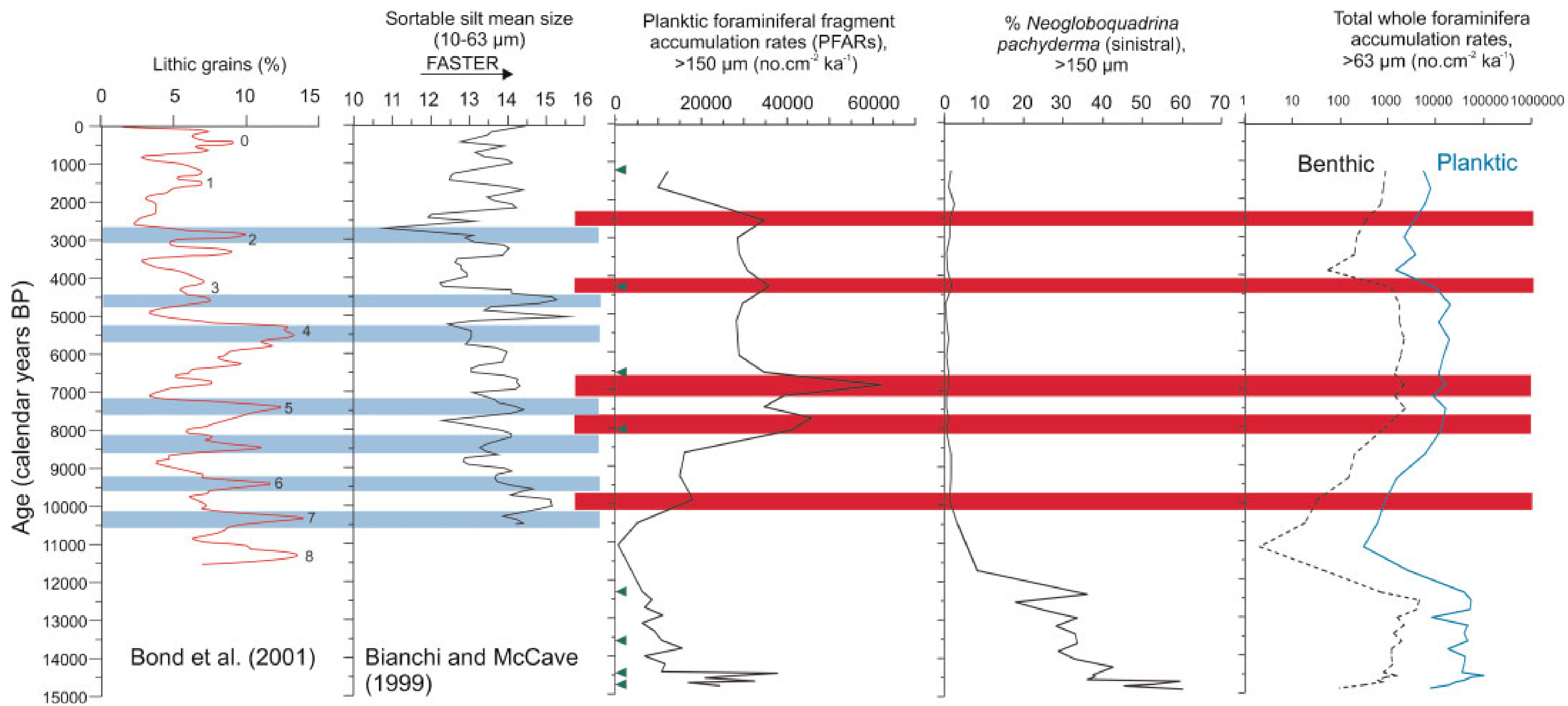

Figure 3 Accumulation rates (number of specimens cm^{-2} ka^{-1}) of planktic foraminiferal fragments (PFAR) (>150 µm), percentage *Neogloboquadrina pachyderma* (sinistral coiling, >150 µm), and total whole planktic and benthic foraminifera (>63 µm) (note the logarithmic scale) (Smart, 2008) during the last 15 ka at BENGAL site 13078#16. Sample positions of AMS radiocarbon analyses are shown (triangles). The accumulation rate data are compared with published Holocene North Atlantic records of percentage lithic grains in the 63–150 µm size range, which reflects the amount of ice-rafted debris, with numbers referring to identified cycles (Bond *et al.*, 2001) and sortable silt mean size in the 10–63 µm size range, which is a palaeocurrent speed proxy (Bianchi and McCave, 1999). Five peaks occur in PFAR (dark horizontal bars) which occur ca. 500 a after the 'Bond' ice rafting events (light horizontal bars). This figure is available in colour online at www.interscience.wiley.com/journal/jqs

productivity is the primary influence on foraminiferal accumulation rates and has no affect on the PFAR. Hence the lack of correspondence between the changes in benthic foraminiferal species and foraminiferal accumulation rates with the PFAR (Fig. 2) suggests dissolution is the major control over the last 12 ka on fragmentation at this site. It has been argued that productivity declines during large freshwater inputs and reduced thermohaline circulation in the North Atlantic (Schmittner, 2005). However, there does not appear to be a relationship between productivity changes and 'Bond' ice rafting pulses at our study site during the Holocene that may be due to localised changes of deep-water sources.

Figure 3 compares the BENGAL foraminiferal fragmentation counts with the Bond *et al.*'s (2001) IRD data and with the Bianchi and McCave's (1999) sortable silt palaeocurrent speed proxy record. This allows us to compare periods of enhanced AABW incursion into the deep North Atlantic Ocean with periods of increased North Atlantic ice rafting and reductions in the speed and circulation of NADW. As discussed above, like our age model, Bond *et al.* (2001) and Bianchi and McCave (1999) used AMS ^{14}C dates on *Globigerina bulloides* and *Globorotalia inflata* to calculate ages after applying 400 a reservoir corrections. Figure 3 illustrates the relationship between IRD, meltwater and reduction in the formation of NADW, which have been suggested by previous authors for millennial-scale cycles in the Holocene (Bond *et al.*, 1997, 2001; Bianchi and McCave, 1999). The BENGAL PFAR record is a proxy for dissolution and this we suggest can be interpreted as indicating the relative carbonate corrosivity of the bottom waters at this site. Because AABW is under-saturated with respect to calcium carbonate water mass compared to the NADW, any increase in PFAR can be attributed to increased incursion of AABW. We speculate that peaks in the PFAR are caused by shoaling of AABW. The youngest two PFAR peaks also correspond to wet periods recorded in southern Chile at 2.8–2.3 and 4.5–4 cal. ka BP (Moreno *et al.*, 2009), suggesting a link between Antarctic climate, AABW formation and the climate of southern South America. Unfortunately, this excellent lake record does not as yet extend further back than 5 ka, so it is not possible to ascertain whether this is a consistent relationship. In addition to the five main dissolution peaks observed in the deep North Atlantic Ocean there is a significant drop in dissolution between 2.5 and 2. cal. ka BP that may represent a significant deepening of the NADW in the late Holocene. Though there seems to be a correspondence between five of the 'Bond' IRD peaks and the PFAR presented, there are two notes of caution. First, the low-resolution nature of the PFAR record, which for part of the record is approximately 400 a, may introduce aliasing, producing a force correlation with the other published records. Second it should be noted that there are no peaks in PFAR associated with 'Bond' IRD peaks 6 and 4. This is most likely due to the relatively low sampling resolution of BENGAL Kasten core 13078#16, but it could also be that there was little or no response of the AABW to these events. However, a much higher-resolution record is required before this can be determined.

Conclusion

Comparison of the timing of the 'Bond' IRD events (Bond *et al.*, 2001) and the reduction of NADW (Bianchi and McCave, 1999) with the PFAR peaks (Fig. 3) suggests there is a 500 a lag between the two records. This may suggest a Holocene bipolar climate seesaw, because if the depth of the AABW in the North East Atlantic Ocean were solely controlled by the amount of NADW being produced, then there should be little or no time lag between records of NADW strength and dissolution proxy. In contrast, there is a clear ca. 500 a lag between these two records. This implies that the strength of the AABW is increasing incrementally subsequent to the reduced NADW strength. This means that the position of the AABW with respect to the NADW is not responding to the reduction in NADW production caused by the meltwater input. Our data therefore indicate that there is very likely a delayed or lagged climatic link between North East Atlantic surface water conditions and AABW production in the Southern Ocean. We suggest that changes in the flow patterns of deep-water masses may be the controlling factor in enhancing AABW production when NADW production has significantly reduced (Seidov *et al.*, 2001). The 500a lag is approximately the timescale that heat exchange from the Northern to Southern Hemisphere would operate on to produce increase AABW production (Schmittner *et al.*, 2003; Knutti *et al.*, 2004). Hence the lag between NADW and AABW during the Holocene is evidence of the bipolar climate seesaw operating during interglacials as well as glacial periods. However, we note that the scale of increase in dissolution as shown by the PFAR is relatively small, particularly considering that a deep site close to the water mass boundary has been chosen for this study. This suggests that although the Holocene bipolar climate seesaw may exist, its climate impact may be relatively small. If we are to find more evidence for the Holocene bipolar climate seesaw we will need to select very sensitive locations to pick up this subtle influence. We must also consider what effects the existence of an interglacial bipolar climate seesaw may have on predictions of future climate.

Acknowledgements We thank Andy Gooday (National Oceanography Centre, Southampton, UK) for providing the samples used in this study and Pieter Grootes (Christian-Albrechts University, Kiel, Germany) for running the AMS radiocarbon analyses. CWS gratefully acknowledges financial support from a Royal Society research grant. We would like to thank the two referees for their comments and support.

References

Berger WH, Bonneau M-C, Parker F-L. 1982. Foraminifera on the deep-sea floor: lysocline and dissolution rate. *Oceanologia Acta* **5**: 249–258.

Bianchi GG, McCave IN. 1999. Holocene periodicity in North Atlantic climate and deep-ocean flow south of Iceland. *Nature* **397**: 515–517.

Billett DSM, Rice AL. 2001. The BENGAL programme: introduction and overview. *Progress in Oceanography* **50**: 13–25.

Blunier T, Brook EJ. 2001. Timing of millennial-scale climate change in Antarctica and Greenland during the last glacial period. *Science* **291**: 109–112.

Blunier T, Chappellaz J, Schwander J, Dällenbach A, Stauffer B, Stocker TF, Raynaud D, Jouzel J, Clausen HB, Hammer CU, Johnsen SJ. 1998. Asynchrony of Antarctic and Greenland climate change during the last glacial period. *Nature* **394**: 739–743.

Broecker WS. 1998. Paleocean circulation during the last deglaciation: a bipolar seesaw? *Paleoceanography* **13**: 119–121.

Bond G, Showers W, Cheseby M, Lotti R, Almasi P, deMenocal P, Priore P, Cullen H, Hajdas I, Bonani G. 1997. A pervasive millennial-scale cycle in North Atlantic Holocene and glacial climates. *Science* **278**: 1257–1266.

Bond G, Kromer B, Beer J, Muscheler R, Evans MN, Showers W, Hoffman S, Lotti-Bond R, Hajdas I, Bonani G. 2001. Persistent solar influence on North Atlantic climate during the Holocene. *Science* **294**: 2130–2136.

Broecker WS, Peng TH. 1982. *Tracers in the Sea*. Eldigio Press: New York.

Bronk Ramsey C. 1995. Radiocarbon calibration and analysis in stratigraphy: the OxCal program. *Radiocarbon* **37**: 425–430.

Bronk Ramsey C. 2001. Development of the radiocarbon program OxCal. *Radiocarbon* **43**: 355–363.

Darling KF, Kucera M, Kroon D, Wade CM. 2006. A resolution for the coiling paradox in *Neogloboquadrina pachyderma*. *Paleoceanography* **21**: PA2011.

Denton GH, Broecker WS. 2008. Wobbly ocean conveyor during the Holocene? *Quaternary Science Review* **27**: 1939–1950.

Dickson RR, Brown J. 1994. The production of North Atlantic Deep Water: sources, rates and pathways. *Journal of Geophysical Research* **99**: 12319–12341.

Dittert N, Baumann K-H, Bickert T, Henrich R, Huber R, Kinkel H, Meggers H. 1999. Carbonate dissolution in the deep-sea: methods, quantification and paleoceanographic application. In *Use of Proxies in Paleoceanography: Examples from the South Atlantic*, Fischer G, Wefer G (eds). Springer: Berlin; 255–284.

Gooday AJ. 1988. A response by benthic Foraminifera to the deposition of phytodetritus in the deep sea. *Nature* **332**: 70–73.

Gooday AJ. 1996. Epifaunal and shallow infaunal foraminiferal communities at three abyssal NE Atlantic sites subject to differing phytodetritus input regimes. *Deep-Sea Research* **43**: 1395–1421.

Hemming SR. 2004. Heinrich events: massive late Pleistocene detritus layers of the North Atlantic and their global climate imprint. *Review of Geophysics* **42**: RG1005, 1–43.

Hughen KA, Baillie MGL,Bard E, Beck JW, Bertrand CJH, Blackwell PG, Buck CE, Burr GS, Cutler KB, Damon PE, Edwards RL, Fairbanks RG, Friedrich M, Guilderson TP, Kromer B. McCormac G, Manning S, Ramsey CB, Reimer PJ, Reimer RW, Remmele S, Southon JR, Stuiver M, Talamo S, Taylor FW, Van der Plicht J, Weyhenmeyer CE. 2004. Marine04 marine radiocarbon age calibration, 0–26 cal kyr BP. *Radiocarbon* **46**: 1059–1086.

Knutti R, Flückiger J, Stocker TF, Timmermann A. 2004. Strong hemispheric coupling of glacial climate through freshwater discharge and ocean circulation. *Nature* **430**: 851–856.

Le J, Shackleton NJ. 1992. Carbonate dissolution fluctuation in the western equatorial Pacific during the Late Quaternary. *Paleoceanography* **7**: 21–42.

Maslin M, Seidov D, Lowe J. 2001. Synthesis of the nature and causes of rapid climate transitions during the Quaternary. In *The Oceans and Rapid Climate Change: Past, Present and Future*, Seidov D, Haupt BJ, Maslin M (eds). *Geophysical Monograph* **126**: 9–52.

McCartney MS. 1992. Recirculating components to the deep boundary current of the northern North Atlantic. *Progress in Oceanography* **29**: 283–383.

Moreno PI, Francois JP, Villa-Martinez RP, Moy CM. 2009. Millennial-scale variability in Southern Hemisphere westerly wind activity over the last 5000 years in SW Patagonia. *Quaternary Science Reviews* **28**: 25–38.

Peterson LC, Prell WL. 1985. Carbonate dissolution in recent sediments of the eastern equatorial Indian Ocean: preservation patterns and carbonate loss above the lysocline. *Marine Geology* **64**: 259–290.

Rasmussen TL, Thomsen E. 2004. The role of the North Atlantic Drift in the millennial timescale glacial climate fluctuations. *Palaeogeography, Palaeoclimatology, Palaeoecology* **210**: 101–116.

Sarnthein M, Winn K, Jung SJA, Duplessy J-C, Labeyrie L, Erlenkeuser H, Ganssen G. 1994. Changes in east Atlantic deepwater circulation over the last 30,000 years: eight time slice reconstructions. *Paleoceanography* **9**: 209–267.

Schmidt MW, Vautravers MJ, Spero HJ. 2006. Rapid subtropical North Atlantic salinity oscillations across Dansgaard–Oeschger cycles. *Nature* **443**: 561–564.

Schmittner A. 2005. Decline of the marine ecosystem caused by a reduction in the Atlantic overturning circulation. *Nature* **434**: 628–633.

Schmittner A, Saenko OA, Weaver AJ. 2003. Coupling of the hemispheres in observations and simulations of glacial climate change. *Quaternary Sciences Reviews* **22**: 659–671.

Seidov D, Maslin MA. 1999. Collapse of the North Atlantic Deep water circulation during the Heinrich events. *Geology* **27**: 23–26.

Seidov D, Maslin MA. 2001. Atlantic Ocean heat piracy and the bipolar climate seesaw during Heinrich and Dansgaard–Oeschge events. *Journal of Quaternary Science* **16**: 321–328.

Seidov D, Haupt BJ, Barron EJ, Maslin M. 2001. Ocean bi-polar seesaw and climate: southern versus northern meltwater impacts. In *The Oceans and Rapid Climate Change: Past, Present and Future*, Seidov D, Haupt BJ, Maslin M (eds). Geophysical Monograph **126**: 147–167.

Smart CW. 2008. Abyssal NE Atlantic benthic foraminifera during the last 15 kyr: relation to variations in seasonality of productivity. *Marine Micropaleontology* **69**: 193–211.

Stocker TF. 1998. The seesaw effect. *Science* **282**: 61–62.

Sun X, Corliss BH, Brown CW, Showers WJ. 2006. The effect of primary productivity and seasonality on the distribution of deep-sea benthic foraminifera in the North Atlantic. *Deep-Sea Research I* **53**: 28–47.

Thunell RC. 1976. Optimum indices of calcium carbonate dissolution in deep-sea sediments. *Geology* **4**: 525–528.

van Aken HM. 2000. The hydrography of the mid-latitude Northeast Atlantic Ocean. I. The deep water masses. *Deep-Sea Research I* **47**: 757–788.

Vidal L, Labeyrie L, Cortijo E, Arnold M, Duplessy JC, Michel E, Becqué S, van Weering TCE. 1997. Evidence for changes in the North Atlantic Deep Water linked to meltwater surges during the Heinrich events. *Earth and Planetary Science Letters* **146**: 13–19.

Volbers ANA, Henrich R. 2002. Calcium carbonate corrosiveness in the South Atlantic during the Last Glacial Maximum as inferred from changes in the preservation of *Globigerina bulloides*: a proxy to determine deep-water circulation patterns? *Marine Geology* **204**: 43–57.